Influence of additional electric field on discharge performance of Hall thruster under internal and external cathode position studied by particle-in-cell simulation

IEPC-2019-285

Presented at the 36th International Electric Propulsion Conference
University of Vienna • Vienna, Austria
September 15-20, 2019

Xifeng Cao[1], Hui Liu[2], Daren Yu[3]
Laboratory of Plasma Propulsion, Harbin Institute of Technology (HIT), Harbin, Heilongjiang, 150001, China

Abstract: In this paper, PIC-MCC simulation method is used to simulate the discharge process of Hall thruster under the internal and external cathode conditions with additional electric field. This paper compares the variation of parameters such as electric potential during the discharge of thruster under internal and external cathode conditions. Under the internal cathode condition, the potential distribution in plume region is relatively high. At the same time, the potential near the central axis is relatively high. Comparing the two-dimensional distribution of ions, it is found that under the internal cathode condition, the ionization region is relatively outside, and the peak densities of Xe^{2+} and Xe^{3+} ions are relatively low. The statistics of plume divergence angle show that under the internal cathode condition, plume divergence angle is relatively low and plume convergence effect is better. By comparing the results of plume calculation under the additional electric field, it is shown that the additional electric field can effectively reduce the plume divergence angle. Under the condition that the additional electric field is on the outer upper side, the plume divergence angle can be reduced by 37.64% under the internal cathode condition and 39.29% under the external condition. By comparing the ion flux bombarding on the magnetic pole surface, it can be found that the additional electric field has little effect on the ion bombarding on the magnetic pole surface under the external cathode condition, but has a noticeable effect under the internal cathode condition.

Nomenclature

Δt	=	time step
ω_{pe}	=	electron oscillation frequency
ω_c	=	electron cyclotron frequency
f	=	coefficient to increase the mass of a heavy particle
γ	=	coefficient to increase the vacuum permittivity
I_d	=	discharge current
w	=	real number of particles represented by simulated particles
Δn_i^c	=	number of ions ejected from the channel at the last moment

[1] Ph. D student, Laboratory of Plasma Propulsion, 1058458931@qq.com.
[2] Associate professor, Laboratory of Plasma Propulsion, thruster@126.com.
[3] Professor, Laboratory of Plasma Propulsion, yudaren@hit.edu.cn.

Δn_e^c	=	number of electrons ejected from the channel at the last moment
n	=	plasma density
v_e	=	electron velocity
m_e	=	electron mass
φ	=	electric potential
$\boldsymbol{B}$	=	magnetic induction intensity
T_e	=	electron temperature
l	=	direction of magnetic induction line

I. Introduction

THe Hall thruster has the advantages of high specific impulse, long life, compact structure, small volume and less pollution. It has been widely used in satellite location maintenance, attitude adjustment, orbit change, resistance compensation and many interplanetary missions.[1-5] Hall thruster has an annular channel. The radial magnetic field is formed in the channel due to the inside and outside electric coils and permanent magnet structure. The axial electric field is formed by the potential difference between the anode and the cathode. The electrons are bound by the magnetic field, and the electrons drift along the axis under the orthogonal electromagnetic field. The propellant (usually xenon) is ionized into plasma by electrons, and ions are accelerated to form thrust, as shown in Fig. 1.[6] Due to factors such as the electric field in the radial direction, the ions have a radial velocity, so they will diffuse to the sides after the ions are accelerated to eject, and finally form a plume divergence angle (the plume divergence angle is considered to account for 90% of the total plume). Larger plume divergence angle can cause significant plume pollution, affecting components such as satellite bodies and solar panels

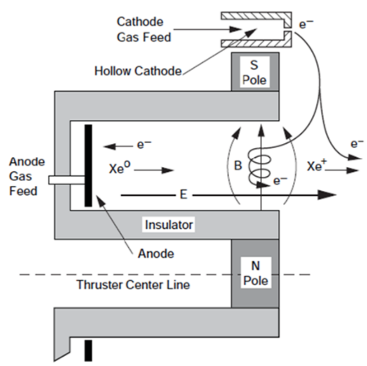

Figure 1. The structure diagram of Hall thruster[6]

At present, many scholars have carried out relevant research on reducing the plume divergence angle of Hall thruster, such as using additional electrodes[7-11] and optimizing cathode power supply.[12,13] These methods can effectively reduce plume divergence angle, but there are also some drawbacks. There are two main methods for the treatment of additional electrodes, one is to add an additional electrode in the channel, the other is to add additional electrodes in the plume region.[7,14] At present, the research of additional electrodes is mainly focused on the interior of thruster, trying to improve the performance of thruster by changing the ionization inside the channel, but this method can not effectively reduce the plume divergence angle. Compared with the built-in additional electrodes, the external electrodes are directly applied to the plume region, which provides the possibility for the direct adjustment of particle distribution in the plume region. However, there are relatively few studies on the additional electrodes in the plume region. In the experiment, Gridwords et al. tried to add electrodes in the plume region. By adjusting the electric field and magnetic field in the plume region, the plume divergence angle decreased.[14] However, the additional electrodes in the plume region will affect the electric field distribution in the near-field plume region, which may aggravate the bombardment on the surface of the magnetic pole surface. However, there are few theoretical studies on the external additional electrodes at this stage, and the above problems still need to be further studied. In addition, as far as the external additional electrodes are concerned, most of the current studies focus on the structure of the external cathode thruster. As far as the internal cathode structure is concerned, the influence of the external additional electrodes on the performance of the thruster is still unclear, and it is still a problem worth exploring.

In this paper, the influence of additional electric field on discharge parameters of Hall thruster under the internal and external cathode conditions is studied by PIC-MCC simulation method. The difference of parameter distribution under the internal and external cathode conditions is compared, and the influence of additional electric field on thrust and plume divergence angle is analyzed. The rest of this paper is organized as follows: the second part introduces the computational model, and the third part discusses the results and analysis of numerical simulations. Finally, the fourth part of the conclusion.

II. Numerical model

A. Particle-in-cell method

As the thruster is an axisymmetric structure, in this paper we use a two-dimensional (2D) simulation. The simulation area includes the anode, channel, near-field plume area. In the simulation we use the particle-in-cell (PIC) simulation method, which simulates the movement of atoms, electrons and ions. The Monte Carlo method (MCC) is used to simulate the collision between particles. The elastic, excitation, single ionization and multiple ionization collisions between electrons and atoms are considered in the model. The Poisson equation is used to solve the electric field. The magnetic field generated by plasma is much smaller than the applied magnetic field generated by the coils. Thus, the magnetic field generated by plasma is neglected. This model has been used to study hall thruster,[15,16] high efficiency multistage plasma thrusters,[17] near-wall conductivity, [18] power deposition on the wall and erosion.[19] In the simulation, different boundary conditions need to be considered and different treatment methods are selected for different boundary conditions. The boundary conditions are shown in Fig. 2. When the particles hit the metal walls, ions lost their charges and were re-emitted as neutrals, in random directions, with kinetic energies equal to half their initial energies. Electrons were removed, and the neutrals were re-emitted at the same temperature as the wall. When particles hit the anode, the electrons were deleted, and their charges were conducted or deposited. The atoms inherited the temperature of the anode surface and were re-emitted from the anode surface. The ions were recombined into atoms by electrons, and the new generated atoms were re-emitted at half the energy of the initial ions. The particles emitted by the anode surface were in the form of a half-Maxwellian distribution. When particles hit the dielectric walls, the ions were neutralized by the negative charges accumulated on the walls, becoming atoms. These new generated atoms were then re-emitted at the half-Maxwellian velocity into space, with half the energy of the original ions. The atoms inherited the temperature of the dielectric wall and were uniformly emitted into the hemispherical space with a half-Maxwellian distribution. As the dielectric wall of the Hall thruster is usually made of BN ceramic, the secondary electron emission model in Ref. 20 was chosen as the electron and wall collision model. At the center line, the particles were reflected specularly. Any type of particle motion was considered to disappear through the free-space boundary, and the corresponding particle was deleted in the program. The cathode adopts a stable discharge model, in which the discharge current of the thruster is constant.[21] Discharge current consists of electron current and ion current. The ion current can be calculated by counting the number of ions ejected from the thruster channel. Therefore, the number of injected electrons Δn_e at each time can be calculated by the ion current and the given discharge current. I_d is 3 A in this paper.

The specific expression is as follows

$$\Delta n_e = \frac{I_d \Delta t}{ew} - \Delta n_i^c - \Delta n_e^c \tag{1}$$

Two cathode position conditions are used in this paper, which are internal cathode and external cathode. In order to fully investigate the movement of electrons emitted from different cathode positions in plume region, the upper and right boundary of plume region are set together as external cathode boundary. The boundary conditions are shown in Fig. 2. The magnetic field used in the simulation is obtained by FEEM software. The design of the general magnetic field is chosen to obtain the peak value of the magnetic field at the channel outlet as shown in Fig. 2. The location of the additional electric field is shown in the Fig. 2. The upper boundary of the plume region is mainly divided into two regions, 0-30 grid and 30-60 grid, respectively. And selecting 20 V as additional potential is mainly to avoid the negative impact of excessive potential on the discharge of thruster.

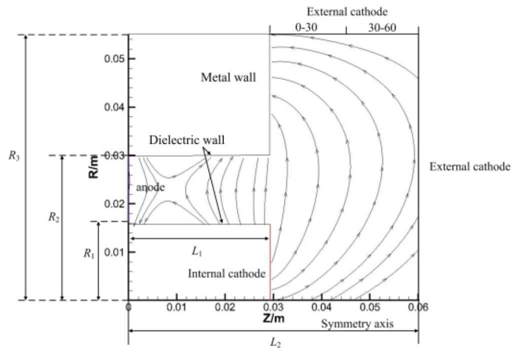

Figure 2. Magnetic field distribution and calculation area, including the anode area, channel, near field plume area. Boundary conditions include dielectric, metal, cathode, free side, symmetry side, metal, dielectric, and anode.

The related parameters are shown in table 1.

Table 1. the calculate area parameters

parameter name	Parameter value
Inner channel radius R_1（mm）	16
Outer channel radius R_2（mm）	29
Calculate area radius R_3（mm）	55
Channel length L_1（mm）	30
Calculate area length L_3（mm）	60
Anode potential（V）	300

The orthogonal grid is used. The size of the grid length is 0.5 mm, which is about 0.5 times the Debye length. The time step Δt equals a smaller value of $0.1\,\omega_{\mathrm{pe}}^{-1}$ and $0.35\,\omega_{\mathrm{c}}^{-1}$. Because the electron oscillation is smaller and the value is about 10^{11} Hz, the time step Δt is taken as 10^{-12} s. In order to reduce the computational complexity of the simulation and accelerate the convergence, many researchers have proposed different simulation simplification methods at present.[22-24] In this paper, a simplified model given by Szabo is selected, which increases vacuum permittivity and reduces the ion mass.[25] And the vacuum permittivity is increased by a factor of γ^2=1600, in order to reduce the number of grids and the plasma oscillation frequency. The ion mass is reduced by a factor $1/f$ =100 so that the velocity of the ions increases by $\sqrt{f}$ times to reduce the time scale by the same amount, and the collision cross-section needs to increase by $\sqrt{f}$ times to preserve the density of plasma in the discharge channel. The feasibility of this method has already been proved in our recent simulation work.[26,27] The simulation is calculated by using a personal computer with the above simplified model. After about a week calculation, convergent results are obtained successfully.

III. Simulation results

A. Potential

Potential distribution is an important parameter of Hall thruster. The acceleration to ions by the potential directly determines the distribution of thrust and plume divergence angle of the thruster. First, we compare the two-dimensional distribution of potential under the internal external conditions, as shown in Fig. 3. By comparison, it can be found that the potential distribution in plume region is obviously different under the two conditions. Under the internal cathode condition, the potential distribution in plume area is relatively high, the potential at the outlet is about 100V under the internal cathode condition, and 60V under the external cathode condition. At the same time, under the external cathode condition, the potential distribution is symmetrical along the central axis of the channel. While under the internal cathode condition, the potential near the symmetrical axis is relatively high. From the center axis of the outlet, the potential decreases gradually along the magnetic field line to both sides. The distribution of magnetic induction lines and potential lines can be explained by the equation of motion of electrons.

The equation of motion of the electron is shown in Eq. (2).

$$nm_{\mathrm{e}}\frac{\mathrm{d}\boldsymbol{v}_{\mathrm{e}}}{\mathrm{dt}}=en\nabla\varphi-en\boldsymbol{v}_{\mathrm{e}}\times\boldsymbol{B}-\nabla\left(nkT_{\mathrm{e}}\right)-nkT_{\mathrm{e}}\frac{1}{B}\nabla B \tag{2}$$

The first term on the right side of the equation is the electric field term, and the second is the Lorentz force term, and the third is the electronic pressure term, and the fourth is the magnetic mirror effect term. Under steady-state conditions, the left side of the equation is 0. The electrons in the plume region can be considered to move along the magnetic induction line (the simulation of the trajectory of the electrons can be explained), so the Lorentz force term along the magnetic induction line is 0. Along the magnetic induction line, the equation of motion of electrons can be simplified as shown in Eq. (3).[28]

$$\frac{d\varphi}{dl}=\frac{kT_e}{eB}\frac{dB}{dl}+\frac{kT_e}{en}\frac{dn}{dl} \tag{3}$$

It can be seen from Eq. (3) that the variation of the potential along the induction line is determined by the electron pressure term and the magnetic mirror effect term. Because the magnetic field in the plume region is small and the magnetic field intensity along the magnetic field line varies little, the change of electric potential on the magnetic field line is mainly determined by the electron pressure. At the same time, because the electron density on the axis of the thruster is relatively high and diffuses toward both sides, the density decreases gradually. Therefore, the electron pressure term is obviously negative, so along the magnetic field line the potential gradually decreases toward both sides. The distribution of potential is shown in the Fig. 3. In order to better illustrate, we make a numerical analysis of the potential distribution on the inductance line. We selected two points A and B on the magnetic field line with internal cathode, as shown in the following Fig. 3. Point A is the intersection of the channel midline and the magnetic field line, and point B is the intersection of the magnetic field line and the 40V isopotential line. These two points are selected mainly because the main beam region is the focus of our investigation. The potential drop in this region is relatively large, and the magnetic field line along AB is relatively collimated, and the calculation error is small. The simulation results show that the potential value at point A is 54.58 V, the electron density is $3.88\times10^{17}/\mathrm{m}^3$, the magnetic field intensity is 0.021 T, the potential value at point B is 40 V, the electron density is $1.42\times10^{17}/\mathrm{m}^3$, the magnetic field intensity is 0.017 T, and the average temperature is 13.5 eV. The calculated results show that the potential decrease caused by the electron pressure term is about 13.5 V, and the potential decrease caused by the change of magnetic field is 2.7 V. The total potential decreases to 16.2 V, slightly higher than the simulated potential drop. Therefore, it can be considered that the potential distribution satisfies the thermalization potential theory, and the change of the potential along the magnetic field line is mainly determined by the electronic pressure.

At the same time, under the internal cathode condition, the electrons emitted from the cathode increase the electron density near the central line, the decrease of the electron density becomes slower, and the value of the electron pressure term is relatively small, which leads to a relatively high potential in the area below the central line of the channel. As shown in the Fig. 3, the potential near the upper boundary of plume region is close to 0 V, while the potential near the boundary of symmetrical axis can reach more than 20 V, which is consistent with the analysis results.

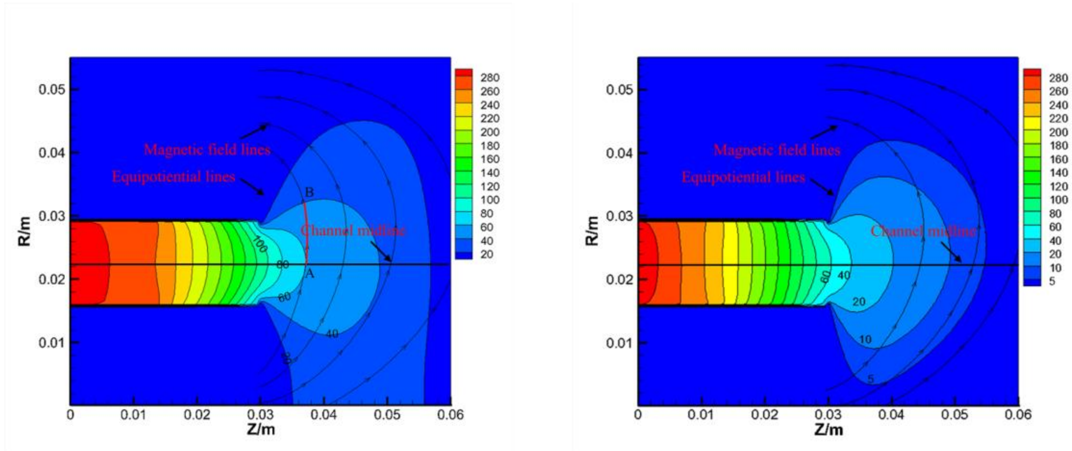

a) internal **b) external**

Figure 3. Two-dimensional distribution of potential under the internal and external cathode conditions

Further, the potential distribution under the additional electric field is compared. Because the two-dimensional distribution is close, the potential changes on the central axis of the channel are compared, as shown in the Fig. 4. Case 0-30 and Case 30-60 correspond to the case that the additional electric field is loading at the regions of 0-30 grid and 30-60 grid, respectively. It can be found that the potential near the anode decreases slowly under the internal cathode condition, because the ionization region is relatively outward under this condition. And the potential change inside the channel is relatively large under the external cathode condition because the ionization region is relatively close to the anode. At the same time, it can be found that the additional electric field has a relatively large effect on the potential distribution on the central axis under the internal cathode condition, but has little effect under the external cathode condition.

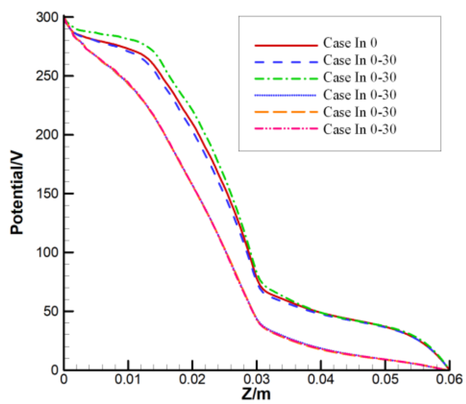

Figure 4. The potential along the central axis of channel under the different conditions

In order to further compare the radial potential in the plume region, we select the potential distribution in radial direction at Z=45 mm and Z=60 mm, which are the boundary of the additional electric field. And the selected radial range is above the thruster outlet as R=28~55 mm, as shown in Fig. 5. Through comparison, it can be found that the potential under the internal condition is relatively high.

Meanwhile, the potential decreases gradually from the center of the channel to both sides. The effect of the additional electric field on the position near the channel is relatively small, and its effect mainly concentrates near the upper boundary. In order to further analyze the effect of additional electric field on the discharge of thruster, the distribution of radial electric field in plume region is compared, as shown in the Fig. 6. It can be found that the additional electric field has a great influence on the radial electric field, and the additional electric field can effectively improve the electric field intensity near the upper boundary. At the same time, it can be found that the additional electric field has a greater impact on the radial electric field under Case 30-60. The maximum electric field strength can reach 25000 V/m. The increase of the radial electric field can inhibit the diffusion of ions to both sides and help to reduce the plume divergence angle.

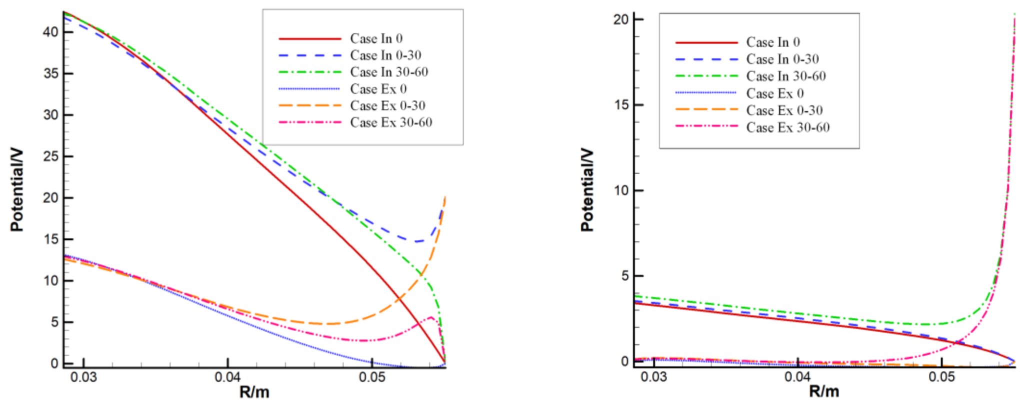

a) **b)**

Figure 5. the distribution of the potential in radial direction (a) Z=45 mm (b) Z=60 mm

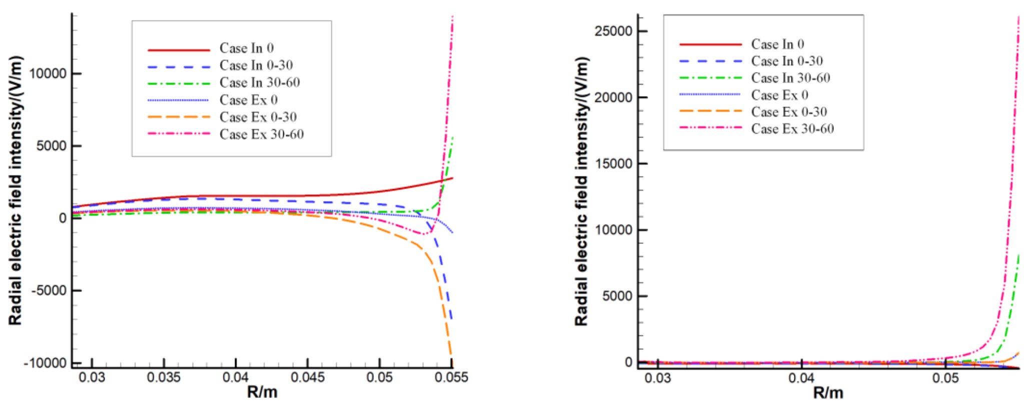

a) **b)**

Figure 6. the distribution of the radial electric field in radial direction (a) Z=45 mm (b) Z=60 mm

B. Ion density

Changing the additional electric field has little effect on the ion distribution, so only the two-dimensional distributions of Xe^{+}, Xe^{2+} and Xe^{3+} ions under the internal and external conditions are shown in Fig. 7. By comparison, it is found that under two conditions, the density of Xe+ ions is relatively high, and the density of Xe^{3+} ions is low. After counting under the internal cathode conditions, the ratio of Xe^{+} ions to total ions is 91.62%, and the ratio of Xe^{2+} and Xe^{3+} ions is 7.65% and 0.73%, respectively. Under the external cathode conditions, the ratio of Xe^{+} ions to total ions was 88.39%, and the ratio of Xe^{2+} and Xe^{3+} ions was 10.64% and 0.97%, respectively. The ratio is basically consistent with the measurement results in the literature 29. At the same time, as the valence state increases, the ion peak position gradually moves outward along the channel. This is because the high-valence ions are generated by the collision of high-energy electrons and atoms or the collision of electrons and low-valence ions. So, the location is relatively outward.

At the same time, it can be found that under the internal cathode condition, the ionization region of the three kind ions is relatively outside. This is due to the relatively high potential near the outlet under the internal cathode condition, as shown in Fig. 3. The ionization rate of working gas $R_{ion} = n_e n_a \beta_i$, n_e is the electron density, n_a is the atomic density and β_i is the ionization velocity coefficient which is directly determined by the electron temperature.

Under the internal cathode condition, electrons can obtain higher energy near the channel outlet, so under the internal cathode condition, the ionization regions of Xe^{+}, Xe^{2+} and Xe^{3+} ions are relatively outside. At the same time, due to the relatively low atomic density near the outer side, the density of Xe^{2+} and Xe^{3+} ions under the internal cathode condition is relatively low, and the axial broadening of the ionization region is significantly increased.

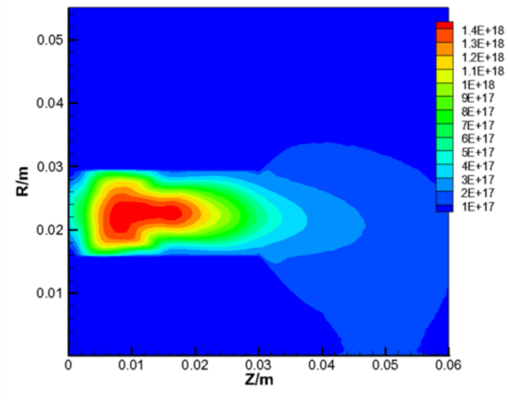

a)Two-dimensional distribution of Xe^{+} ions

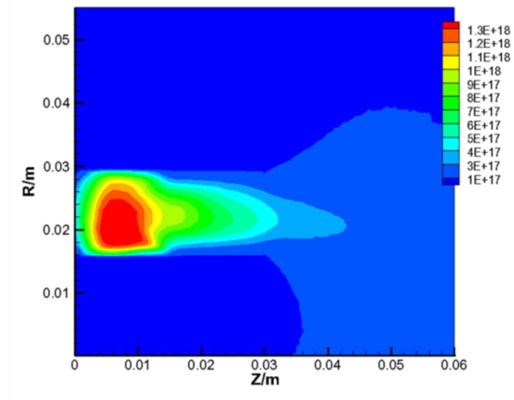

b) Two-dimensional distribution of Xe^{+} ions

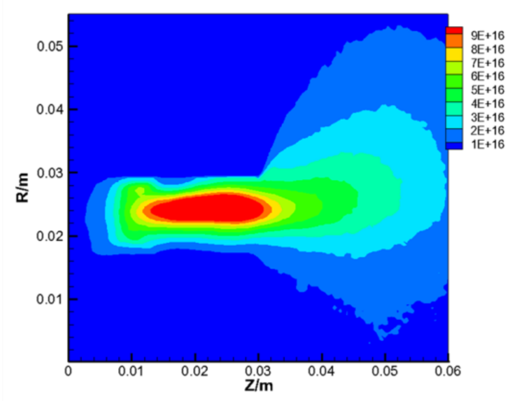

c) Two-dimensional distribution of Xe^{2+} ions

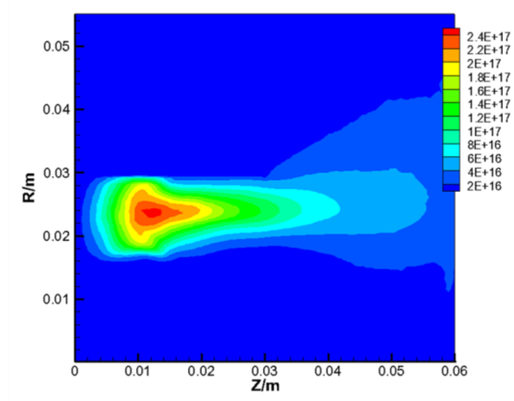

d) Two-dimensional distribution of Xe^{2+} ions

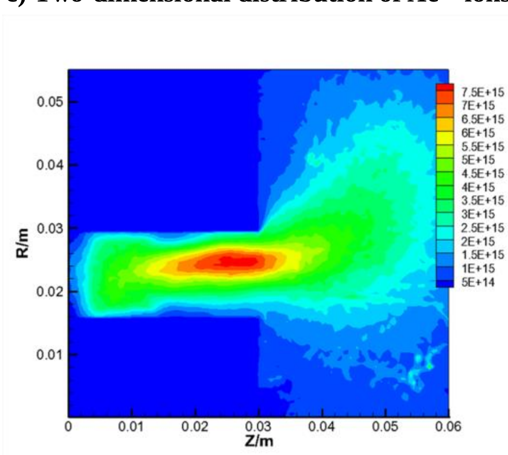

e) Two-dimensional distribution of Xe^{3+} ions

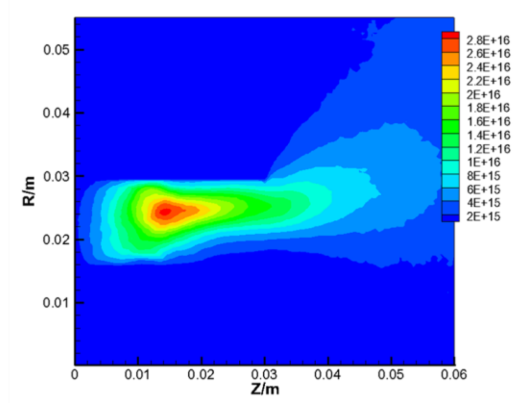

f) Two-dimensional distribution of Xe^{3+} ions

Figure 7. Two-dimensional distribution of Xe^{+}, Xe^{2+} and Xe^{3+} under internal and external cathode conditions a), c), e) internal b), d), f) external

The plume divergence angle under the internal and external cathode conditions with additional electric field is calculated. The half divergences angle under the different conditions are shown in the table 2. The half divergence angle under the internal cathode condition is 36.95 degrees, and the half divergence angle under the external cathode condition is 37.13 degrees, which is consistent with the previous experimental measurements (39.5~37.5 degrees).[30] The results show that the plume convergence effect is relatively better under the internal cathode condition, which is consistent with the conclusions obtained in previous experiments.[31,32]
At the same time, it can be found that the additional electric field can effectively reduce the divergence angle of the plume. In particular, the additional electric field has a significant convergence effect on the divergence angle of the plume under the condition of 30-60, which is related to the large external boundary electric field. A larger electric field can effectively suppress the diffusion of ions to the outside of the thruster, thereby reducing the divergence angle of the plume.

Table 2. the plume divergence angle under the different conditions

	Case 0	Case 0-30	Case 30-60
Internal	36.95	27.74	23.04
External	37.13	36.68	22.54

C. Ion Flux on the magnetic pole surface

Previous studies have shown that there exists ion bombardment on the magnetic pole surface of the thruster in the near field plume region, and that changing the potential of the magnetic pole will affect the ion bombardment. Therefore, this section further compares the ion bombardment on the magnetic pole surface on both sides under the internal and external cathode conditions and additional electric fields, as shown in Fig. 8. It can be found that the magnetic pole surface is heavily bombarded by ions. This is due to the fact that some electrons will move towards the inner magnetic pole bound by magnetic field, which results in relatively more ionization of atoms. Further comparison shows that the ion bombardment is relatively more under the internal cathode condition, which is due to the more ionization of atoms at the cathode boundary. At the same time, comparing the ion flux under different additional electric field conditions, it can be found that the existence of additional electric field can enhance the ion flux on the magnetic pole surface. Under the internal cathode condition, the additional electric field has a great influence on the ion flux on the external magnetic pole surface. This is because the existence of an additional electric field can attract electrons to move towards the upper boundary and enhance the ionization in this region. This effect is more significant under the internal cathode condition.

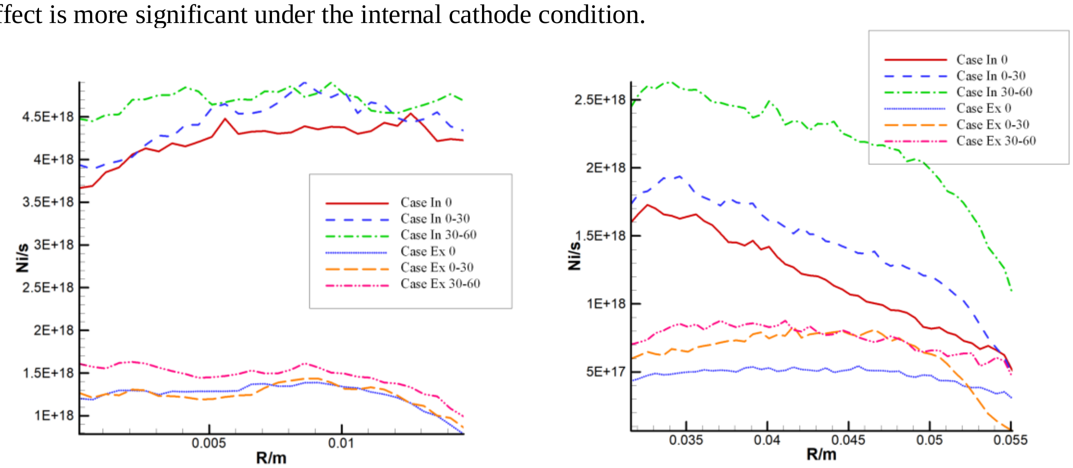

a) inner magnetic pole surface **b) outer magnetic pole surface**

Figure 8. The ion bombardment on the magnetic pole surface under internal and external cathode conditions

IV. Conclusion

In this paper, PIC-MCC simulation method is used to simulate the discharge process of Hall thruster under the internal and external cathode conditions. This paper compares the variation of parameters such as electric potential during the discharge of thruster under internal and external cathode conditions. Under the internal cathode condition, the potential distribution in plume region is relatively high. At the same time, the potential near the central axis is relatively high. By comparing the radial distribution of potential and electric field in plume region, it can be found that the existence of additional electric field can enhance the potential and electric field near the upper boundary. The enhancement of electric field is helpful to inhibit ion diffusion to both sides and reduce plume divergence angle. Comparing the two-dimensional distribution of ions, it is found that under the internal cathode condition, the ionization region is relatively outside, and the peak densities of Xe^{2+} and Xe^{3+} ions are relatively low. The statistics of plume divergence angle show that under the internal cathode condition, plume divergence angle is relatively low and plume convergence effect is better. By comparing the results of plume calculation under the additional electric field, it is shown that the additional electric field can effectively reduce the plume divergence angle. The plume divergence angle can be reduced by 37.64% under the condition of internal cathode and 39.29% under Case 30-60. By comparing the ion flux bombarding on the magnetic pole surface, it can be found that the additional electric field has little effect on the ion bombarding on the magnetic pole surface under the external cathode condition, but has a noticeable effect under the internal cathode condition.

References

[1]Vatistas, G. H., Lin, S., and Kwok, C. K., "Reverse Flow Radius in Vortex Chambers," *AIAA Journal*, Vol. 24, No. 11, 1986, pp. 1872, 1873.

[1]Mazouffre, S., "Electric propulsion for satellites and spacecraft: established technologies and novel approaches.," *PLASMA SOURCES SCI T*, Vol. 25, No. 3, 2016, 033002.

[2]Boeuf, J. P., "Tutorial: Physics and modeling of Hall thrusters," *J APPL PHYS*, Vol. 121, No. 1, 2017,011101.

[3].Kim, H., Choe, W., Lim, Y., Lee, S., and Park, S., "Magnetic field configurations on thruster performance in accordance with ion beam characteristics in cylindrical Hall thruster plasmas," *APPL PHYS LETT*, Vol. 110, No. 11, 2017, 114101.

[4]Goebel, D. M., Hofer, R. R., Mikellides, I. G., Polk, J. E., and Dotson, B. N., "Conducting wall Hall thrusters," *IEEE T PLASMA SCI*, Vol. 43, No. 1, 2014, pp. 118-126.

[5]Yuge, S., and Tahara, H., "Performance Enhancement of a 1-kW Anode-layer Hall Thruster," in Proceedings of the 29th International Electric Propulsion Conference, Princeton, IEPC-2005-20, 2005.

[6]Goebel, D. M., and Katz, I., Fundamentals of electric propulsion: ion and Hall thrusters, John Wiley & Sons, New Jersey, 2008, pp. 6.

[7]Griswold, M. E., Raitses, Y. and Fisch, N. J., "Plasma lens focusing of the hall thruster plume," in Proceedings of the 32nd International Electric Propulsion Conference, Germany, IEPC-2011-177, 2011.

[8]Gabor, D., "A space-charge lens for the focusing of ion beams," *Nature*, Vol. 159, No. 4055, 1947, 89.

[9]Morozov, A. I., "Focussing of Cold Quasineutral Beams in Electromagnetic Fields," *Dokl.akad.nauk Sssr*, Vol. 10, No. 6, 1965, pp. 1363-1366.

[10]Goncharov, A. A., Zatuagan, A. V., and Protsenko, I. M., "Focusing and control of multiaperture ion beams by plasma lenses," *IEEE Trans. Plasma Sci*, Vol. 21, No. 5, 1993, 0-581.

[11]Goncharov, A., Dobrovolsky, A., Protsenko, I., Kaluh, V., Onishenko, I., and Brown, I., "Reverse Flow Radius in Vortex Chambers," *REV SCI INSTRUM*, Vol. 69, No. 2, 1998, 1135.

[12]Granstedt, E. M., Raitses, Y., and Fisch, N. J., "Cathode effects in cylindrical hall thrusters," *J APPL PHYS*, Vol. 104, No. 10, 2008, 103302.

[13]Yu, D. R., Meng, T. H., Ning, Z. X., and Liu, H., "Confinement effect of cylindrical-separatrix-type magnetic field on the plume of magnetic focusing type Hall thruster," *PLASMA SOURCES SCI T*, Vol. 26, No. 4, 2017, 04LT02.

[14]Griswold, M. E., Raitses, Y., and Fisch, N. J., "Cross-field plasma lens for focusing of the Hall thruster plume," *PLASMA SOURCES SCI T*, Vol. 23, No. 4, 2014, 044005.

[15]Liu, H., Yu, D. R., Yan, G. J., and Liu, J. Y., "Investigation of the start transient in a Hall thruster," *CONTRIB PLASM PHYS*, Vol. 48, No. 9-10, 2008, pp. 603-611.

[16]Liang, S. T., Liu, H., and Yu, D. R., "Particle-in-cell simulation for the effect of magnetic cusp on discharge characteristics in a cylindrical Hall thruster," *CHINESE PHYS B*, Vol. 27, No. 4, 2018, 045201.

[17]Liu, H., Chen, P. B., Sun, Q. Q., Hu, P., Meng, Y. C., Mao, W., et al., "Design of a cusped field thruster for drag-free flight," *ACTA ASTRONAUT*, Vol. 126, 2016, pp. 35-39.

[18]Yu, D., Li, H., Wu, Z., and Mao, W., "Effect of oscillating sheath on near-wall conductivity in Hall thrusters," PHYS PLASMAS, Vol. 14, No. 6, 2007, 064505.

[19]Cao, X. F., Hang, G. R., Liu, H., Meng, Y. C., Luo, X. M., and Yu, D. R., "Hybrid - PIC simulation of sputtering product distribution in a Hall thruster," *PLASMA SCI TECHNOL*, Vol. 19, No. 10, 2017, 105501.

[20]Yu, D. R., Zhang, F. K., Liu, H., Li, H., Yan, G. J., and Liu, J. Y., "Effect of electron temperature on dynamic characteristics of two-dimensional sheath in Hall thrusters," *PHYS PLASMAS*, Vol. 15, No. 10, 2008, 104501.

[21]Liu, H., "Study on characteristics of electron behaviours in Hall thrusters," Ph.D. Dissertation, HIT, Harbin, China, 2009.

[22]Fox, J. M., "Advances in fully-kinetic PIC simulations of a nearvacuum Hall thruster and other plasma systems," Ph.D. Dissertation, MIT, Boston, USA, 2007.

[23]Fife, J. M., "Hybrid-PIC modeling and electrostatic probe survey of Hall thrusters," Ph.D. Dissertation, MIT, Boston, USA, 1999.

[24]Parra, F. I., and Ahedo, E., "A two-dimensional hybrid model of the Hall thruster discharge," *J APPL PHYS*, Vol. 100, No. 2, 2006, 023304.

[25]Szabo, J. J., "Fully kinetic numerical modeling of a plasma thruster," Ph.D. Dissertation, MIT, Boston, USA, 2001.

[26]Zhao, Y. J., Liu, H., Yu, D. R., Hu, P., and Wu, H., "Particle-in-cell simulations for the effect of magnetic field strength on a cusped field thruster," *J PHYS D APPL PHYS*, Vol. 47, No. 4, 2013, 045201.

[27]Liu, H., Chen, P. B., Zhao, Y. J., and Yu, D. R., "Particle-in-cell simulation for different magnetic mirror effects on the plasma distribution in a cusped field thruster," *CHINESE PHYS B*, Vol. 24, No. 8, 2015, 085202.

[28]Keidar, M., and Boyd, I. D., "On the magnetic mirror effect in Hall thrusters," *APPL PHYS LETT*, Vol. 87, No. 12, 2005, 121501.

[29]King, L. B., and Gallimore, A. D., "Mass spectral measurement in the plume of an SPT-100 Hall thruster," J PROPUL POWER, Vol. 16, No. 6, 2000, pp. 1086-1092.

[30]Ding, Y., Su, H., Li, H., Jia, B. Y., Wei, L. Q., Peng, W. J., et al., "Measurement method for plume divergence angle of Hall thrusters," *J VAC SCI TECHNOL B*, Vol. 37, No. 1, 2019, 012902.

[31]Hofer, R. R., Johnson, L. K., Goebel, D. M., Wirz, R. E., "Effects of internally mounted cathodes on Hall thruster plume properties," *IEEE T PLASMA SCI*, Vol. 36, No. 5, 2008, pp. 2004-2014.

[32]McDonald, M. S., and Gallimore, A. D., "Cathode position and orientation effects on cathode coupling in a 6-kW Hall thruster," in Proceedings of the 31th International Electric Propulsion Conference, USA, IEPC-2009-113, 2009.